INFECTION AND IMMUNITY, Sept. 1999, p. 4700–4707 Vol. 67, No. 9
0019-9567/99/$04.00+0

Preliminary Characterization of a *Mycobacterium abscessus* Mutant in Human and Murine Models of Infection

THOMAS F. BYRD[1,2]* AND C. RICK LYONS[2]

Department of Medicine, Albuquerque Veterans Affairs Medical Center,[1] and The University of New Mexico School of Medicine,[2] Albuquerque, New Mexico 87108

Received 9 March 1999/Returned for modification 7 April 1999/Accepted 18 June 1999

The ability to persist in the host after the establishment of infection is an important virulence determinant for mycobacteria. *Mycobacterium abscessus* is a rapidly growing mycobacterial species which causes a variety of clinical syndromes in humans. We have obtained a rough, wild-type human clinical isolate of *M. abscessus (M. abscessus-R)* and a smooth, attenuated mutant *(M. abscessus-S)* which spontaneously dissociated from the clinical isolate. We have found that *M. abscessus-R* is able to persist and multiply in a murine pulmonary infection model in contrast to *M. abscessus-S*, which is rapidly cleared. To understand the basis for this difference, we characterized the behavior of these variants in human tissue culture models of infection. *M. abscessus-R* is able to persist and multiply in human monocytes, while *M. abscessus-S* is deficient in this ability. Both of these variants are phagocytized by human monocytes. *M. abscessus-R* resides in a phagosome typical for pathogenic mycobacteria with a tightly adherent phagosomal membrane. In contrast, *M. abscessus-S* resides in a "loose" phagosome with the phagosomal membrane separated from the bacterial cell wall. Both *M. abscessus* variants also have distinctive growth patterns in a recently described fibroblast-mycobacterium microcolony assay, with *M. abscessus-R* exhibiting growth characteristics similar to those previously reported for virulent *M. tuberculosis* and *M. abscessus-S* exhibiting growth characteristics similar to those previously reported for avirulent *M. tuberculosis*. In both the monocyte infection assay and the murine pulmonary infection model, numerous infected mononuclear phagocyte aggregates develop at sites of *M. abscessus-R* infection, but are absent with *M. abscessus-S* infection. We conclude that a mutation has occurred in the *M. abscessus-S* variant which has altered the ability of this organism to persist and multiply in host cells and that this may be related to the phenotypic changes we have observed in our tissue culture models of infection.

Mycobacterial diseases are significant causes of morbidity and mortality. Non-tuberculous mycobacteria are being increasingly identified in clinical specimens (31). *Mycobacterium abscessus* is a rapidly growing mycobacterial species which causes a variety of clinical syndromes in humans (31), including skin and soft tissue infection, disseminated infection, lymphadenitis, postoperative catheter-related infection, and bone and joint infection. *M. abscessus* was formerly considered to be a subspecies of *Mycobacterium chelonae* (*M. chelonae* subsp. *abscessus*), but on the basis of DNA homology studies it has been shown to be genetically distinct and has thus been elevated to a separate species status (29). Its increasing clinical importance is highlighted by the fact that its has recently been described to cause a well-characterized chronic bronchopulmonary infection similar to that caused by *Mycobacterium avium* (15, 25).

In addition to their significance as human pathogens, nontuberculous mycobacteria have been used as models to study the pathogenesis of infection caused by mycobacteria in general. For example, *Mycobacterium marinum* infection of the leopard frog (*Rana pipiens*) has been used as a model of mycobacterial pathogenesis because of its similarity to tuberculosis. In this model, *M. marinum* causes a nonlethal chronic granulomatous disease in immunocompetent frogs. Immunosuppression associated with hydrocortisone treatment results in acute fulminant, lethal disease (26). In addition, *M. marinum* infection of macrophages has been used as a model to study intracellular trafficking of mycobacteria. In one study, *M. marinum* localized to a similar intracellular vacuole as *M. tuberculosis* (2). Finally, because of similarities of *M. tuberculosis* and *Mycobacterium leprae*, *M. marinum* has been used to study the oxidative stress response of pathogenic mycobacteria (24).

To aid in our study of mycobacterial pathogenesis, we have obtained a rough, wild-type isolate of *M. abscessus* (*M. abscessus-R*) and a smooth, attenuated mutant (*M. abscessus-S*) which spontaneously dissociated from a single human clinical isolate. In this study we show that *M. abscessus-R* is able to persist in a murine pulmonary model of infection in contrast to *M. abscessus-S*, which is not. As a first step toward characterizing the basis for mycobacterial persistence, we have identified phenotypic differences between these variants in human tissue culture models of infection.

MATERIALS AND METHODS

Mycobacterial strains. *M. abscessus* variants were obtained from Blaine Beaman at The University of California, Davis. *M. abscessus-R* was isolated in pure culture from an ileal granuloma in a patient with Crohn's disease. This form induced granuloma formation in both the ileum and colon of goats (2a). *M. abscessus-S* was a spontaneous mutant of the rough colony strain isolated in vitro (2a). To support the observation that *M. abscessus-R* and *M. abscessus-S* are derived from the same isolate, additional studies were performed. Both variants have essentially identical elution patterns on high-pressure liquid chromatography (HPLC) identifying them as *M. abscessus*, and other *M. abscessus* strains show greater differences in their elution patterns when compared to these two variants, supporting their close identity (11a). In addition to forming nonpigmented colonies and having a rapid growth rate, biochemical analysis showed both these variants to be *M. abscessus* (nitrate reduction negative, positive for growth in 5% NaCl, iron uptake negative, citrate negative, inositol negative, and mannitol negative). Restriction enzyme analysis was performed after PCR amplification of a portion of the gene encoding for the 65-kDa heat shock protein. Using the restriction endonucleases *Bst*EII and *Hae*III, both isolates were found to be identical to the *M. abscessus* control strain. Finally, random amplified

* Corresponding author. Mailing address: Department of Medicine (111J), Albuquerque Veterans Affairs Medical Center, 1501 San Pedro, SE, Albuquerque, NM 87108. Phone: (505) 265-1711, extension 2488. Fax: (505) 256-2803. E-mail: tfbyrd@pol.net.

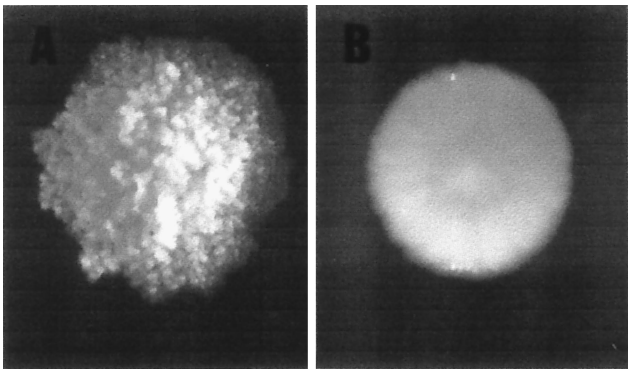

FIG. 1. Morphologic appearance of *M. abscessus-R* (left) and *M. abscessus-S* (right) colonies. These are 7-day-old colonies on 7H11 agar.

polymorphism detection was performed on both variants. In this technique, short primers with arbitrary sequences and nonstringent PCR conditions are used to generate variable-length fragments which vary according to the sequence of the isolates being tested. Identical patterns for *M. abscessus-R* and *M. abscessus-S* were obtained by using two separate reactions with different random primers supporting the close genetic identity of these variants (13a).

These variants have remained stable through 10 passages in bacterial culture media. Furthermore, in eight separate infection experiments in mice, each using both variants, we have not observed a change in colony morphology of either *M. abscessus-R* or *M. abscessus-S* recovered from the lung or spleen, further attesting to phenotypic stability of these variants.

Bacterial culture media. Middlebrook 7H9 broth (Difco, Detroit, Mich.) was used for the dilution of culture supernates and lysates prior to plating for CFU. Middlebrook 7H11 agar (Difco) plates (100- by 15-mm bacteriologic petri dishes) were used for plating CFU from infected monolayers and supernates.

Mice. Female BALB/c and SCID mice were obtained from The Jackson Laboratory, Bar Harbor, Maine. Animals were maintained in a specific-pathogen-free environment. The animal colonies were screened regularly for the presence of murine pathogens.

Murine pulmonary infection assay. *M. abscessus* used in these experiments was the second passage of bacteria originally received from B. Beaman. *M. abscessus* was grown in 100 ml of 7H9 broth, harvested by centrifugation, and resuspended in phosphate-buffered saline (PBS)–Tween. Bacteria were then sonicated in an ultrasonic cell disrupter (Microson XL; Heat Systems, Farmingdale, N.Y.) to disperse organisms, and any remaining clumps allowed to settle for 15 min. The supernatant was then removed, aliquoted, and flash frozen. A new aliquot was used for each experiment. Prior to inoculation into animals, *M. abscessus* suspensions were sonicated for 30 s to ensure a uniform bacterial suspension.

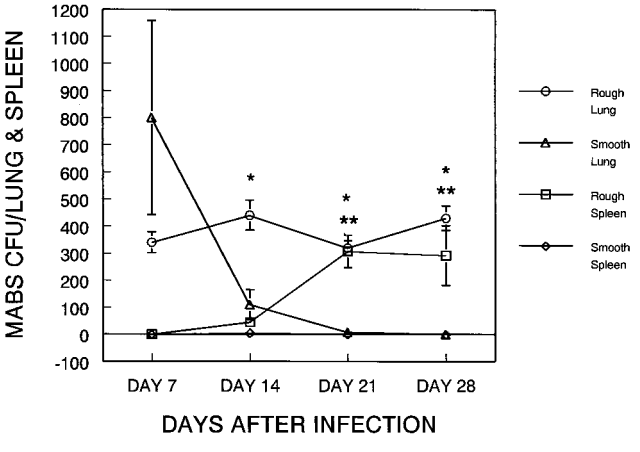

FIG. 2. In a murine pulmonary model of infection, *M. abscessus-R* persists in both the lung and spleen and disseminates to the spleen, whereas *M. abscessus-S* is rapidly cleared and does not disseminate. SCID mice ($n = 4$) were intratracheally inoculated with 10^4 *M. abscessus-R* or *M. abscessus-S* organisms. At the indicated time intervals, the mice were sacrificed and the total lung and spleen CFU values were determined. The data represent the mean ± the standard deviation. *, *M. abscessus-R* versus *M. abscessus-S* in the lung ($P < 0.05$); **, *M. abscessus-R* versus *M. abscessus-S* in the spleen ($P < 0.05$) (*t* test).

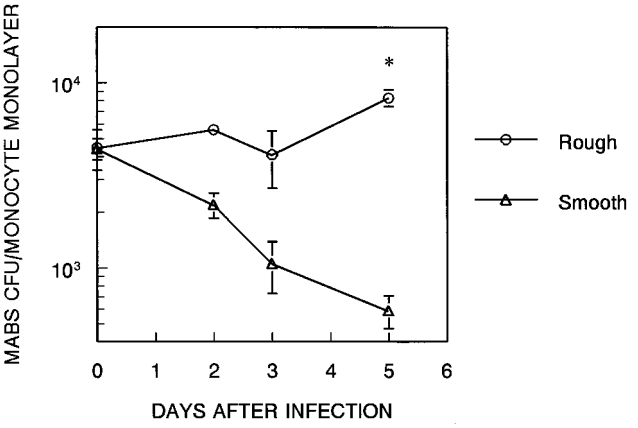

FIG. 3. *M. abscessus-R* persists and multiplies in human monocyte monolayers in contrast to *M. abscessus-S*. Human monocyte monolayers were infected with 2.5×10^5 *M. abscessus-R* or *M. abscessus-S* for 6 h. After being washed, cell lysates and supernatants were plated for CFU at the indicated intervals. CFU in supernatants were less than 5% of the CFU in lysates at all points. Data are the mean of duplicate determinations of two separate experiments. *, *M. abscessus-R* versus *M. abscessus-S* ($P < 0.002$; t test).

Mice were anesthetized by using an intraperitoneal injection of Avertin. An incision was made over the trachea of anesthetized, restrained mice. With a 30-gauge bent needle and syringe, 50 μl of *M. abscessus-R* or *M. abscessus-S* bacterial suspensions containing 10^4 CFU in nonpyrogenic saline was injected into the trachea, and the incision was closed with Super Glue. At various time points after infection (days 7, 14, 21, and 28), mice were sacrificed and the lungs and spleens removed and placed in 3.0 ml of PBS. The organs were homogenized, and dilutions were plated in triplicate by the microdrop technique. Briefly, 25 μl of the dilution was placed as a drop on Middlebrook 7H11 agar. The drops were then allowed to absorb into the agar before incubation in a humidified incubator at 37°C in 10% CO_2 for 2 to 4 days. After incubation the microcolonies are counted by using a stereomicroscope. In addition to CFU, histopathologic sections were obtained and stained with hematoxylin and eosin in order to examine the histology of *M. abscessus*-infected lungs.

Human cells. Human blood mononuclear cells were obtained from buffy coats purchased through United Blood Services (Albuquerque, N.M.). The blood mononuclear cell fraction was obtained by centrifugation over a Ficoll-sodium diatrizoate solution (Pharmacia Fine Chemicals, Piscataway, N.J.), and monocytes were plated as previously described (9).

Tissue culture media. Iscove's modified Dulbecco's medium (Gibco Laboratories, Grand Island, N.Y.) was used in tissue culture experiments.

Serum. Venous blood was obtained from healthy adult volunteers with no history of tuberculosis or a positive tuberculin skin test. Serum was separated and stored at −70°C. Autologous or heterologous serum was used in experiments.

Assay for growth of *M. abscessus* in human monocytes. Human monocytes adherent to Linbro tissue culture wells in Iscove's medium–1% normal human serum (NHS) were incubated for 24 h in 5% CO_2–95% air at 37°C. Frozen bacterial stocks of the *M. abscessus* variants which had been sonicated and preopsonized in normal human serum as previously described for *M. tuberculosis* (9) were used to prepare inoculating suspensions of bacteria for use in each tissue culture experiment. Bacteria frozen were the second passage of *M. abscessus* originally received from B. Beaman. Monolayers were infected with 2.5×10^5 *M. abscessus-R* or *M. abscessus-S* for 6 h and then washed three times with media. A time zero count was plated, and then amikacin at 30 μg/ml was added to the tissue culture medium to kill any remaining extracellular bacteria. After 48 h the monolayers were washed three times with medium, and amikacin not re-added. Subsequently, at 24-h intervals, the monolayers were washed twice with medium to prevent bacterial overgrowth in the medium by extracellular bacteria. Platings for supernate and lysate CFU were performed at 48, 72, and 120 h as previously described for *M. tuberculosis* (9). Similar results were obtained either by vortexing the bacteria in Eppendorf tubes containing three glass beads or by sonicating the bacteria with an ultrasonic cell disrupter prior to plating. In some experiments, the growth of the *M. abscessus* variants was assessed by a radiometric method that measured microbial metabolism (18). Infected *M. abscessus-R* and *M. abscessus-S* monocyte lysates in 0.5-ml aliquots were inoculated into BACTEC 12B bottles containing 7H12 Middlebrook broth (Becton Dickinson, Sparks, MD) and the growth index determined daily by using a BACTEC 460 instrument (Becton Dickinson, Sparks, Md.). In all experiments, monocyte viability was also analyzed in replicate infected wells by trypan blue exclusion as

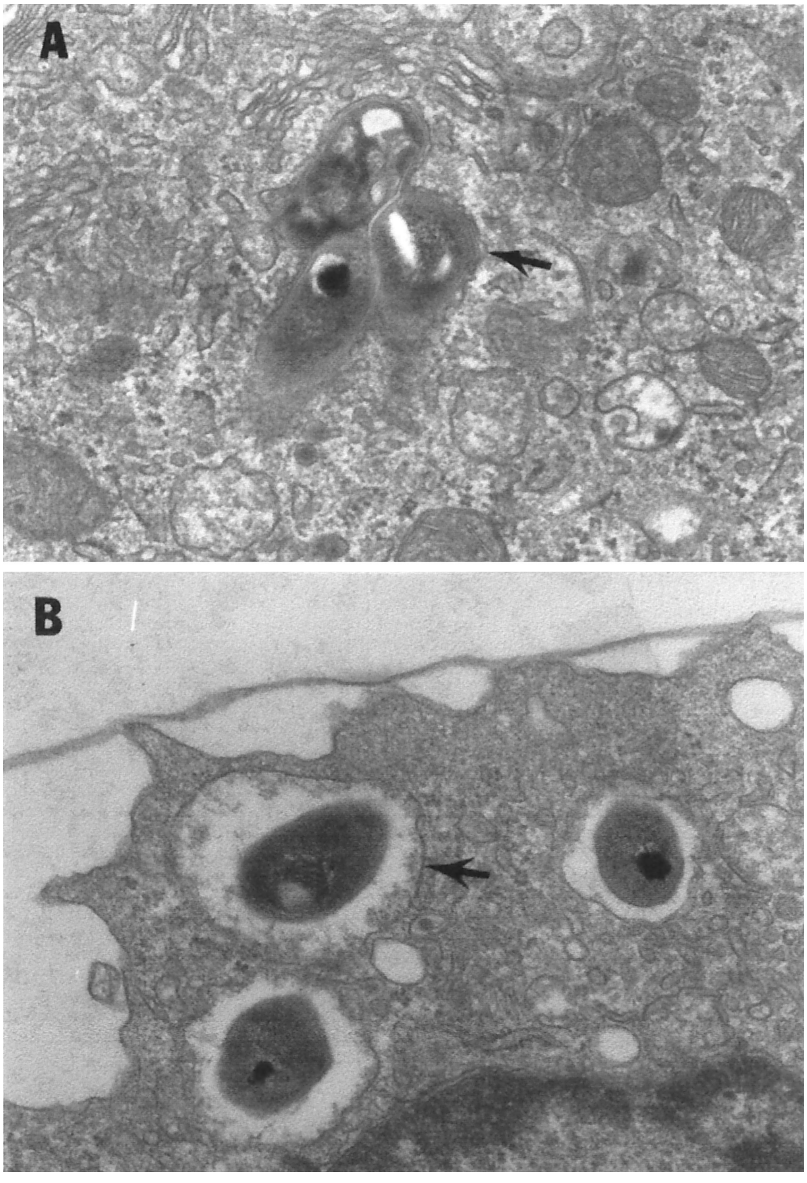

FIG. 4. *M. abscessus* variants are phagocytized by human monocytes and reside in phagosomes with differing morphology. Human monocyte monolayers were incubated with 10^6 *M. abscessus-R* or *M. abscessus-S* for 1 h, followed by washing and an additional 30 min of incubation to allow for internalization of bacteria. Electron microscopy was then performed. Fifteen consecutive phagosomes were identified for each group, containing one to four bacteria per monocyte. All bacteria were within monocytes. (A) Three *M. abscessus-R* in a phagosome typical for pathogenic mycobacteria with a tightly adherent phagosomal membrane (arrow). (B) Three *M. abscessus-S* organisms in separate "loose" phagosomes with the phagosomal membrane separated from the bacterial cell wall (arrow). Magnification, ×12,000.

previously described (9) to ensure that the two variants did not have a differential effect on monocyte viability independent of bacterial growth.

Fibroblast-mycobacterium microcolony assay. Fibroblast monolayers were prepared as previously described (10). After fibroblast monolayers had become confluent (3 to 6 days), the wells were washed three times with Iscove's medium, and Iscove's medium alone was re-added. After a 24-h equilibration period, the wells were inoculated with various concentrations of *M. abscessus-R* or *M. abscessus-S* prepared from stock cultures as described above. After a 1-h incubation at 37°C in 5% CO_2–95% air, the monolayers were washed three times with 37°C Iscove's medium, and 3.0 ml of 50 to 52°C Iscove's medium-agar (Difco) overlay was added to each well. After the overlay was hardened at room temperature, the plates were incubated in a humidified incubator at 37°C in 5% CO_2–95% air. Fibroblast monolayers were shown to be viable, as assessed by the addition of a 0.5-ml agar overlay containing neutral red, which penetrated the agar and concentrated in the nuclei of viable cells. At various time intervals, microcolonies were visually inspected for microcolony morphology and photographed with a tissue culture microscope (Nikon, Melville, N.Y.). Microcolonies were fixed by adding 3.0 ml of 80% PBS–20% formaldehyde to each well for 24 h, followed by removal of the agar-medium overlay. Ziehl-Neelsen staining (30) was performed, without methylene blue counterstaining, by flooding the bottom of the wells with carbon fuchsin for 5 min, followed by removal and decolorization with acid alcohol. As a final step, the wells were washed several times washes with double-distilled water. Precise quantitation of microcolony morphology was achieved by photographing the stained microcolonies at ×20 by using a tissue culture microscope (Nikon). By using 4-in.-by-6-in. black-and-white prints, the diameter of the individual microcolonies, measured in the longest dimension, was measured and corrected to the actual size in millimeters. Mean microcolony diameters were obtained for *M. abscessus-R* and *M. abscessus-S*.

Electron microscopy. Human monocytes adherent to 60-mm tissue culture-treated dishes (Costar, Cambridge, Mass.) in Iscove's medium–1% NHS were incubated for 24 h in 5% CO_2–95% air at 37°C. Monocytes were then infected with 10^6 *M. abscessus-R* or *M. abscessus-S* for 1 h. The monolayers were then washed three times with 37°C Iscove's media and incubated for an additional 30 min in 5% CO_2–95% air at 37°C to allow for internalization of the bacteria. The monolayers were then fixed with 2.0% glutaraldehyde in 0.1 M cacodylate buffer (pH 7.4) for 30 min, postfixed with 1.0% osmium tetroxide for 30 min at room temperature, stained with uranyl acetate for 30 min at room temperature, dehydrated with ethanol, released from the surface of the tissue culture dishes with

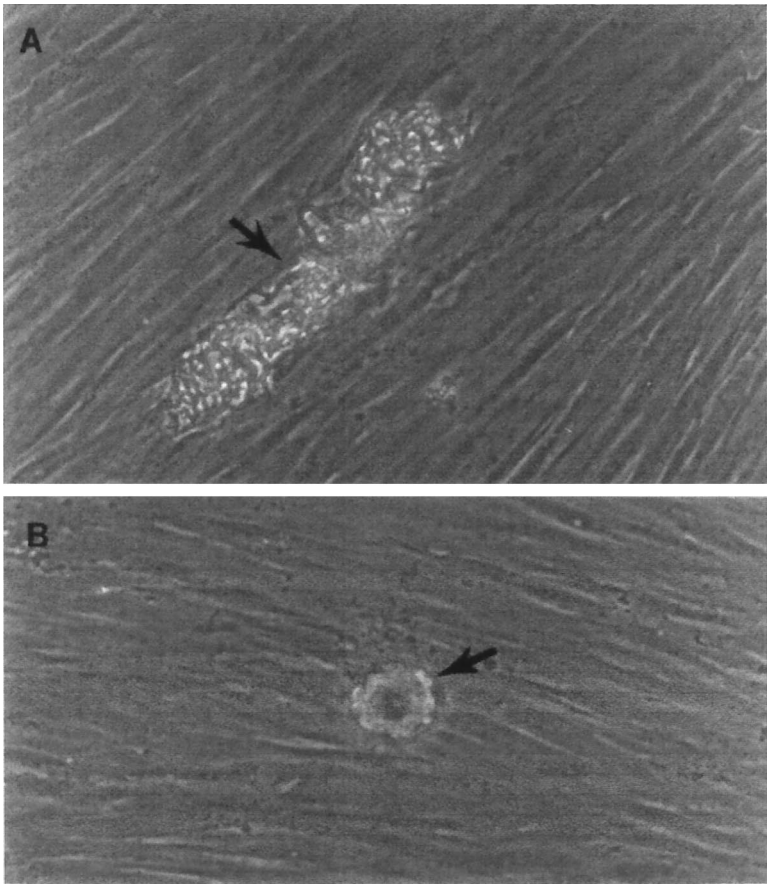

FIG. 5. *M. abscessus* variants form distinctive microcolonies in the fibroblast-mycobacterium microcolony assay. The microscopic appearance of 2-day-old, unfixed, unstained *M. abscessus* growing in human fibroblast monolayers which had been overlaid with agar-tissue culture medium can be seen. (A) *M. abscessus-R*. (B) *M. abscessus-S*. Magnification, ×200.

propylene oxide as previously described (16), and embedded in Epon. Approximately 70-nm-thick sections were stained with uranyl acetate and lead citrate and then examined with a Hitachi H-600 transmission electron microscope.

Confluent human fibroblast monolayers adherent to 60-mm tissue culture-treated dishes in Iscove medium and 5% CO_2–95% air at 37°C were infected with 10^5 *M. abscessus-R* or *M. abscessus-S* for 2 h and then washed three times with 37°C Iscoves medium. The monolayers were then reincubated in 5% CO_2–95% air at 37°C. After 2 days, the monolayers were fixed as described above. In order to examine *M. abscessus* secondarily invading adjacent fibroblasts after primary infection, monolayers were embedded in situ in tissue culture dishes with a thin layer of Epon. After removal of the embedded monolayers, sections approximately 70-nm thick were cut parallel to the original surface of the tissue culture dish, stained with uranyl acetate and lead citrate, and examined with a Hitachi H-600 transmission electron microscope.

Statistics. Data were compared by using the Student's *t* test. Data were considered significant with a P value of <0.05.

RESULTS

***M. abscessus-R* has a rough colony morphology compared to *M. abscessus-S*, which has a smooth colony morphology.** When grown on 7H11 agar plates, *M. abscessus-R* exhibits a colony texture that is rough and dry. In contrast, *M. abscessus-S* exhibits a colony texture that is smooth and moist (Fig. 1).

In a murine pulmonary model of infection, *M. abscessus-S* lacks the ability to persist within the host. To determine whether there are phenotypic differences between *M. abscessus-R* and *M. abscessus-S* in vivo, we infected BALB/c mice with these variants and compared clearance, dissemination, and pathology. *M. abscessus-S* was cleared to undetectable levels, and CFU were never recovered from the spleen. In contrast, *M. abscessus-R* persisted in the lung at 28 days postinfection and was disseminated to the spleen by day 14, although CFU in both the lung and spleen began to decline at day 14 (data not shown). Since the immune response in immunocompetent mice is a major influence on the course of infection and inflammation, we examined the course of infection of these variants in SCID mice which have an immunodeficient B-cell and T-cell response (Fig. 2). We felt infection of these mice would more clearly reflect the innate ability of these variants to persist and elicit inflammation. From day 7 to day 28, *M. abscessus-R* persisted in the lung with little change in CFU over this time period. This ability of *M. abscessus* to persist in the lung was observed in all experiments. Although *M. abscessus-R* disseminated to the spleen in some experiments, this was not as consistent as persistence in the lung and was not observed in all experiments. In contrast, *M. abscessus-S* was rapidly cleared from the lung despite having higher mean CFU levels in the lung at day 7, and no organisms were found in the spleen over the 28-day period of observation (Fig. 2).

***M. abscessus-S* lacks the ability to persist and multiply in human monocyte monolayers.** Human monocyte monolayers were infected with the *M. abscessus* variants, and CFU were assayed over 5 days (Fig. 3). Monocyte monolayers had similar numbers of *M. abscessus-R* and *M. abscessus-S* organisms at time zero. *M. abscessus-R* CFU persisted and multiplied slowly in the monolayer, while *M. abscessus-S* CFU decreased at each successive time point such that there was approximately a 1 log

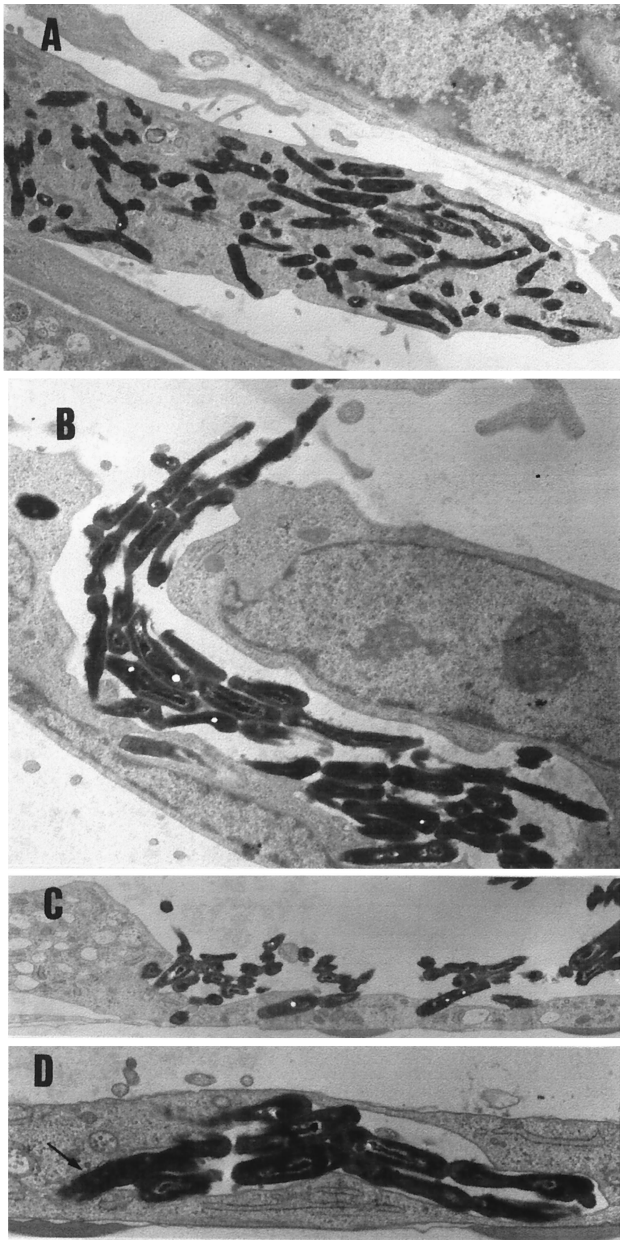

FIG. 6. *M. abscessus-R* multiplies extensively within human fibroblasts and secondarily invades cells after primary infection. (A) Numerous *M. abscessus-R* in fibroblast 2 days after infection. Magnification, ×4,900. (B) *M. abscessus-R* cord effacing and secondarily invading fibroblast. Magnification, ×7,700. (C) *M. abscessus-R* effacing and penetrating the surface of a fibroblast. Magnification, ×4,900. (D) *M. abscessus-R* cord that has been internalized by a fibroblast with bacteria becoming tightly associated with phagosomal membrane (arrow). Magnification, ×9,800. No secondary invasion of fibroblasts by *M. abscessus-S* was identified.

difference between *M. abscessus-R* and *M. abscessus-S* at 5 days (Fig. 3). This divergence between *M. abscessus-R* and *M. abscessus-S* was also noted when *M. abscessus*-infected monocyte lysates from monolayers infected for 0, 48, and 72 h were inoculated into BACTEC 12B culture bottles and the growth index was determined at daily intervals. In this experiment, there was no increase in the growth index of either *M. abscessus-R* or *M. abscessus-S* from 0 to 48 h; however, from 48 to 72 h, the growth index of *M. abscessus-R* increased 310%, whereas the growth index of *M. abscessus-S* increased only 3%. Monocytes remained over 95% viable over the course of all the experiments, indicating that neither variant had a toxic effect on monocytes independent of bacterial growth.

***M. abscessus-R* and *M. abscessus-S* enter human monocytes and reside in morphologically distinct phagosomes.** Similar numbers of the *M. abscessus* variants became associated with the monocyte monolayers at time zero (Fig. 3). To confirm the intracellular location of the variants, electron microscopy was performed on monocytes which had been incubated with either *M. abscessus-R* or *M. abscessus-S*. Electron microscopy showed that both variants are internalized by monocytes but reside in distinctly different phagosomes (Fig. 4).

***M. abscessus-S* has diminished capability to spread from cell to cell in a fibroblast-mycobacterium microcolony assay.** The ability of *M. abscessus-R* and *M. abscessus-S* to invade human fibroblasts was examined. Over a period of 3 to 5 days, these variants formed microcolonies in the fibroblast monolayers which were visible to the naked eye and had distinctive microscopic features (Fig. 5). After acid-fast staining, the mean microcolony diameter and standard deviation of 50 consecutive microcolonies from each variant was determined. *M. abscessus-R* microcolonies had a mean diameter of 0.77 ± 0.15 mm compared to *M. abscessus-S* microcolonies, which had a mean diameter of 0.17 ± 0.12 mm ($P < 0.01$; *t* test).

To confirm the intracellular location of these variants, electron microscopy was performed. Both *M. abscessus-R* and *M. abscessus-S* were taken up by fibroblasts and resided in phagosomes morphologically similar to those seen in infected monocytes. Over a 2-day period, *M. abscessus-R* multiplied extensively within infected fibroblasts and secondarily invaded adjacent fibroblasts (Fig. 6). In contrast, no secondary invasion of fibroblasts by *M. abscessus-S* could be identified.

***M. abscessus-S* lacks the ability to induce the formation of cellular aggregates in the murine pulmonary infection model and in the human monocyte infection model.** In our murine pulmonary infection model with SCID mice, *M. abscessus-R* induced a local inflammatory response identified as discrete collections of macrophages in the lung (Fig. 7), whereas *M. abscessus-S* produced no detectable inflammation. Furthermore, the persistence and multiplication of *M. abscessus-R* in human monocyte monolayers was associated with the development of monocyte aggregates (Fig. 8A). Staining for acid-fast bacilli showed *M. abscessus-R* to be present in these aggregates (data not shown). In contrast, no cellular aggregates were observed in monocyte monolayers infected with *M. abscessus-S* (Fig. 8B).

DISCUSSION

We have obtained an *M. abscessus* human clinical isolate (*M. abscessus-R*) and a spontaneously occurring mutant derived from that isolate (*M. abscessus-S*). Our initial studies indicated that *M. abscessus-R* is able to persist and multiply in our murine pulmonary infection model, whereas *M. abscessus-S* lacks this ability. Using human tissue culture models of infection, we next sought to identify phenotypic differences between these variants which might lead to a further understanding of virulence mechanisms common to pathogenic mycobacteria. Validating the use of these models is our finding that *M. abscessus-S* is also deficient in its ability to persist and multiply in both human monocytes and fibroblasts. We have identified three phenotypic differences between these variants which may play a role in the ability of *M. abscessus-R* to persist and multiply in our murine pulmonary infection model.

The first phenotypic difference, with our human monocyte

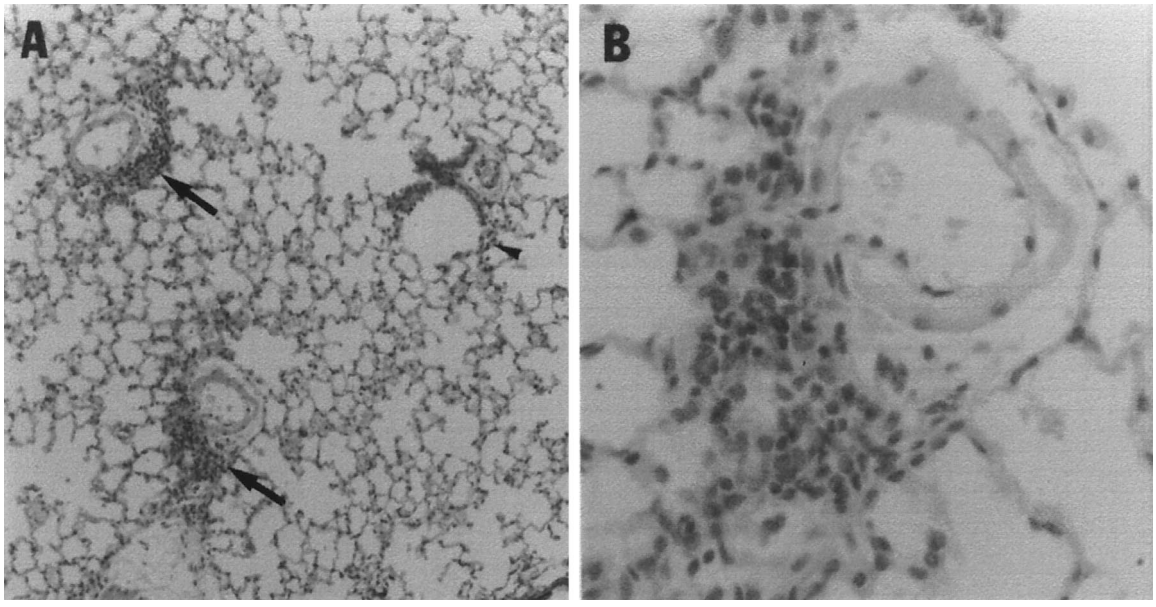

FIG. 7. The lungs of SCID mice infected with *M. abscessus-R* contain numerous inflammatory foci which are absent in the lungs of *M. abscessus-S*-infected mice. (A) Seven days after infection with *M. abscessus-R*. Arrows indicate prominent perivascular inflammatory infiltrates. The arrowhead points to a small number of peribronchiolar inflammatory cells. The tissue was stained with hematoxylin and eosin and photographed at ×25. (B) Enlargement of perivascular inflammatory infiltrate seen in panel A. Magnification, ×100.

infection model, shows that the *M. abscessus* phagosome differs between the two variants. The *M. abscessus-R* phagosome has an appearance typical of that observed for pathogenic mycobacteria, including *M. tuberculosis* (21). The bacterium is surrounded by a tightly adherent phagosomal membrane. The ultrastructure of the bacterial cell wall within the host membrane consists of an outer layer, an electron-transparent layer, and an electron-dense layer, as is also seen in pathogenic mycobacteria. In contrast, *M. abscessus-S* resides in a "loose" phagosome and lacks the typical morphological appearance of the mycobacterial cell wall (8). We speculate on the basis of these findings, that intracellular trafficking of these variants may be different. It has been reported that pathogenic mycobacteria inhibit phagosome-lysosome fusion, thereby avoiding the inhospitable lysosomal environment (1, 2, 12, 14, 23). The difference in persistence between these two variants could in part be due to an inability of *M. abscessus-S* to prevent fusion of its phagosome with lysosomes after entry into host cells. Another explanation could relate to the sensitivity to toxic monocyte metabolites. For example, reactive oxygen intermediates are felt to play a role in bacteriostasis of *M. avium* in a murine model (27). *M. abscessus-R* might be inherently resistant on the basis of an altered cell wall structure, or it might be residing in an intracellular compartment where it would not be exposed to these metabolites. These possibilities are currently under investigation.

The second phenotypic difference pertains to the pattern of growth in our fibroblast-mycobacterium microcolony assay. In the fibroblast-mycobacterium microcolony assay, *M. abscessus-R* forms microcolonies with an elongated appearance

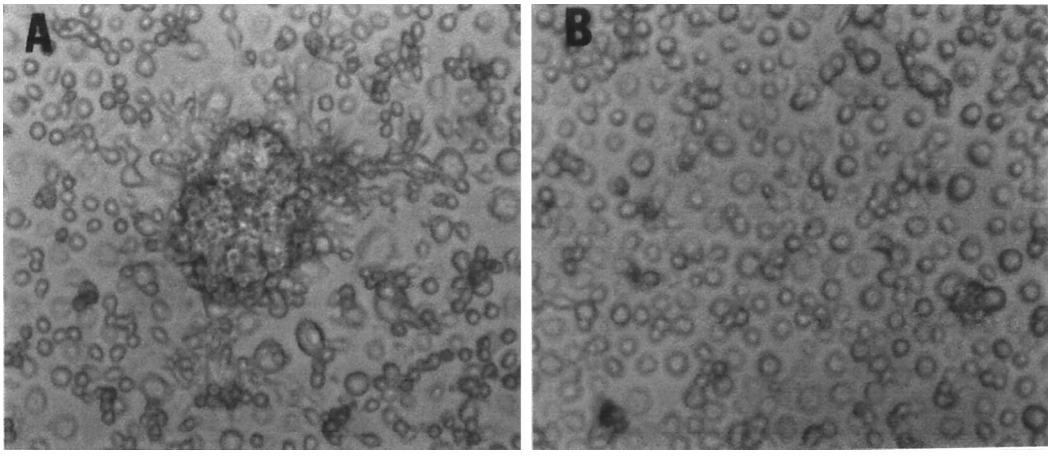

FIG. 8. *M. abscessus-R* infection of human monocytes is associated with the development of monocyte aggregates. Human monocyte monolayers were infected with the *M. abscessus* variants as in Fig. 3. After 3 days, supernatants were removed and the monolayers were examined by trypan blue exclusion. (A) Monolayers infected with *M. abscessus-R* form dense cellular aggregates. (B) Cellular aggregates are completely lacking with *M. abscessus-S*. Magnification (both panels), ×100.

which grow intracellularly in a linear fashion along the long axes of infected fibroblasts and which exhibit extensive cording. With this assay, these characteristics have been shown to differentiate virulent from avirulent *M. tuberculosis* (10). On electron microscopy, *M. abscessus-R* cords can be seen to secondarily invade fibroblasts. In contrast, *M. abscessus-S* forms rounded, noncorded microcolonies which are significantly smaller than *M. abscessus-R* microcolonies. By this assay, these characteristics have been described for the avirulent *M. tuberculosis* strain H37Ra (10). Cording has been postulated to be a virulence factor for various mycobacteria. Middlebrook, as early as 1945, demonstrated that virulent strains of *M. tuberculosis* grow on the surface of liquid media as ropes and coils, whereas avirulent strains appear smooth or wrinkled without a cord-like appearance (19). Two recent studies from this laboratory suggest that cord formation may play a role in the cell-to-cell spread of virulent *M. tuberculosis* (10, 11). The directional movement associated with cord formation may facilitate rapid spread of virulent mycobacteria after host cell death by focusing bacterial growth in one direction. This would allow greater movement by the growing mass of bacteria than would occur in bacteria growing without cord formation. Small distances between cells could be rapidly traversed, with the leading tip of the mycobacterial cord invading new cells and outpacing the cellular immune response, which would be focused on the initially infected, dead, and dying cells. Given the striking similarity between *M. abscessus-R* and virulent *M. tuberculosis* microcolonies on the one hand and *M. abscessus-S* and avirulent *M. tuberculosis* H37Ra microcolonies on the other in the fibroblast-mycobacterium microcolony assay (10), it is possible that cord formation plays an important role in virulence in both of these mycobacterial species.

The third phenotypic difference is the finding that in both human monocyte monolayers and SCID mouse lung, infection with *M. abscessus-R* is associated with the development of monocyte-macrophage aggregates, which are not observed with *M. abscessus-S* infection. In both of these assay conditions, there is a deficiency of T lymphocytes, indicating that *M. abscessus-R* is influencing monocytes directly. Such interaction could be the result of differing cytokine profiles released by mononuclear phagocytes in response to each of these variants. Monocyte-macrophage aggregation may play a role in the pathogenesis of mycobacterial infection. It has been postulated that formation of monocyte aggregates induced by tumor necrosis factor alpha (TNFα) facilitates the cell-to-cell spread of *M. tuberculosis* cords (9). Furthermore, it has been proposed that, although TNF-α is necessary for granuloma formation (17), for *M. tuberculosis* growth restriction to occur the cytokines gamma interferon with interleukin-3 or granulocyte-macrophage colony-stimulating factor are also required to organize the granuloma in such a way that bacterial containment occurs (11). This explanation reconciles the paradox of TNF-α promoting granuloma formation yet at the same time promoting cell-to-cell spread of *M. tuberculosis*. In a similar fashion, formation of monocyte aggregates in response to *M. abscessus-R* could be involved in the pathogenesis of infection with this microorganism.

A common factor which may underlie these three phenotypic differences is the bacterial cell wall. Cord factor (trehalose-6,6′-dimycolate) is present in the cell wall of many mycobacterial species. The role of cord factor in mycobacterial cord formation has been controversial; however, a recent report suggests that cord factor is responsible for the cording phenomenon. In order for cording to occur, trehalose-6,6′-dimycolate molecules must align in a specific orientation (3). Improperly aligned trehalose-6,6′-dimycolate molecules could account for the lack of cord formation observed in avirulent mycobacterial species which contain cord factor. In addition to the studies pertaining to cord factor, there is a substantial body of work which explores the relationship between colony morphology and virulence, as well as the basis for variations in colony morphology within different mycobacterial species (5, 6, 7, 20, 28). Of particular relevance to our study are studies involving *Mycobacterium kansasii*. In one of these studies examining the surface components of rough and smooth colony variants of *M. kansasii* (5), it was observed that the colony morphologies were stable, i.e., smooth colonies were not observed among the rough variants and vice versa. Chemical analysis showed that the rough variants were lacking in lipooligosaccharides. Importantly, the investigators were able to relate this work to an earlier study on the pathogenicity of these *M. kansasii* strains in mice (13), leading to the conclusion that pathogenic strains had a rough phenotype. This finding is consistent with our observations for *M. abscessus-R* and *M. abscessus-S*. In a similar vein, significant progress has been made in revealing the biochemistry and genetic basis for colony morphology in *M. avium*. However, the relevance of these studies to our study is unclear since *M. avium* glycopeptidolipids in the bacterial cell wall are specific to this species and the association between morphology and virulence in *M. avium* has not been well defined (4). Mycobacterial cell wall components have been associated with inflammation and induction of cytokines such as TNF-α; however, with the exception of phenolic glycolipid I of *M. leprae*, which scavenges toxic oxygen radicals generated by activated mononuclear phagocytes (22), there is no data which directly demonstrate a mechanism by which cell wall components of any mycobacterial species play a role in the pathogenesis of infection caused by that species. Using our *M. abscessus* variants and our infection models, future studies will attempt to identify the genetic basis for the persistence phenotype and correlate this with pathogenic mechanisms involved in mycobacterial persistence.

ACKNOWLEDGMENTS

We thank Blaine Beaman for kindly providing the *M. abscessus* variants, Patricia Conville for assistance in the characterization of the variants, and Gary Cage for HPLC analysis of the variants. We are grateful to Jeff Quinn and Donna Kusewitt for expert technical assistance with experiments and to Jan Pfeiffer for expert technical assistance with electron microscopy.

This work was supported by the VA Medical Center, Albuquerque, N.M., and by National Institutes of Health grants AI35249 to T.F.B. and HL55776 to C.R.L. C.R.L. is a Culpeper Medical Scholar, and this work was supported in part by the Culpeper Medical Scholar Foundation.

REFERENCES

1. **Armstrong, J. A., and P. D. A. Hart.** 1975. Phagosome-lysosome interactions in cultured macrophages infected with virulent tubercle bacilli. J. Exp. Med. **142:**1–16.
2. **Barker, L. P., K. M. George, S. Falkow, and P. L. Small.** 1997. Differential trafficking of live and dead *Mycobacterium marinum* organisms in macrophages. Infect. Immun. **65:**1497–1504.

2a. **Beaman, B.** Personal communication.

3. **Behling, C. A., B. Bennett, K. Takayama, and R. L. Hunter.** 1993. Development of a trehalose 6,6′-dimycolate model which explains cord formation by *Mycobacterium tuberculosis*. Infect. Immun. **61:**2296–2303.
4. **Belisle, J. T., M. R. McNeil, D. Chatterjee, J. M. Inamine, and P. J. Brennan.** 1993. Expression of the core lipopeptide of the glycopeptidolipid surface antigens in rough mutants of *Mycobacterium avium*. J. Biol. Chem. **268:** 10510–10516.
5. **Belisle, J. T., and P. J. Brennan.** 1989. Chemical basis of rough and smooth variation in mycobacteria. J. Bacteriol. **171:**3465–3470.
6. **Belisle, J. T., L. Pascopella, J. M. Inamine, P. J. Brennan, and W. R. Jacobs.** 1991. Isolation and expression of a gene cluster responsible for the biosynthesis of the glycopeptidolipid antigens of *Mycobacterium avium*. J. Bacteriol. **173:**6991–6997.

7. **Belisle, J. T., K. Klaczkiewicz, P. J. Brennan, W. R. Jacobs, Jr., and J. M. Inamine.** 1993. Rough morphological variants of *Mycobacterium avium*. Characterization of genomic deletions resulting in the loss of glycopeptidolipid expression. J. Biol. Chem. **268:**10517–10523.
8. **Brennan, P. J., and P. Draper.** 1994. Ultrastructure of *Mycobacterium tuberculosis*, p. 274–277. *In* B. R. Bloom (ed.), Tuberculosis: pathogenesis, protection, and control. ASM Press, Washington, D.C.
9. **Byrd, T. F.** 1997. TNFα promotes growth of virulent *M. tuberculosis* in human monocytes: Iron-mediated growth suppression is correlated with decreased release of TNFα from iron-treated, infected monocytes. J. Clin. Investig. **99:**2518–2529.
10. **Byrd, T. F., G. M. Green, S. E. Fowlston, and C. R. Lyons.** 1998. Differential growth characteristics and streptomycin susceptibility of virulent and avirulent *Mycobacterium tuberculosis* in a novel fibroblast-mycobacterium microcolony assay. Infect. Immun. **66:**5132–5139.
11. **Byrd, T. F.** 1998. Multinucleated giant cell formation induced by IFNγ/IL-3 is associated with restriction of virulent *Mycobacterium tuberculosis* cell to cell invasion in human monocyte monolayers. Cell. Immunol. **188:**89–96.

11a. **Cage, G.** Personal communication.

12. **Clemens, D. L., and M. A. Horwitz.** 1995. Characterization of the *Mycobacterium tuberculosis* phagosome and evidence that phagosomal maturation is inhibited. J. Exp. Med. **181:**257–270.
13. **Collins, F. M., and D. S. Cunningham.** 1981. Systemic *Mycobacterium kansasii* infection and regulation of the alloantigenic response. Infect. Immun. **22:**614–624.

13a. **Conville, P.** Personal communication.

14. **Frehel, C., C. de Chastellier, T. Lang, and N. Rastogi.** 1986. Evidence for inhibition of lysosomal and prelysosomal compartments with phagosomes in macrophages infected with pathogenic *Mycobacterium avium*. Infect. Immun. **52:**252–262.
15. **Griffith, D. E., W. Girard, and R. J. Wallace.** 1993. Clinical features of pulmonary disease caused by rapidly growing mycobacteria. An analysis of 154 patients. Am. Rev. Respir. Dis. **147:**1271–1278.
16. **Griffiths, G., G. Warren, T. Quinn, O. Mathieu-Costello, and H. Hoppeler.** 1984. Density of newly synthesized plasma membrane proteins in intracellular membranes. I. Stereological studies. J. Cell Biol. **98:**2133–2141.
17. **Kindler, V., A. Sappino, G. E. Grau, and P. Piguet.** 1989. The inducing role of tumor necrosis factor in the development of bactericidal granulomas during BCG infection. Cell **56:**731–740.
18. **Meylan, P. R. A., D. D. Richman, and R. S. Kornbluth.** 1992. Reduced intracellular growth of mycobacteria in human macrophages cultivated at physiologic oxygen pressure. Am. Rev. Respir. Dis. **145:**947–953.
19. **Middlebrook, G.** 1945. Pathogenic components of tubercle bacilli. Am. Rev. Tuberc. **51:**244–259.
20. **Mills, J. A., M. R. McNeil, J. T. Belisle, W. R. Jacobs, and P. J. Brennan.** 1994. Loci of *Mycobacterium avium ser2* gene cluster and their functions. J. Bacteriol. **176:**4803–4808.
21. **Moreira, A. L., J. Wang, L. Tsenova-Berkova, W. Hellmann, V. H. Freedman, and G. Kaplan.** 1997. Sequestration of *Mycobacterium tuberculosis* in tight vacuoles in vivo in lung macrophages of mice infected by the respiratory route. Infect. Immun. **65:**305–308.
22. **Neill, M., and S. J. Klebanoff.** 1988. The effect of phenolic glycolipid-1 from *Mycobacterium leprae* on antimicrobial activity of human macrophages. J. Exp. Med. **167:**30–42.
23. **Oh, Y. K., and R. M. Straubinger.** 1996. Intracellular fate of *Mycobacterium avium*: use of dual label spectrofluorometry to investigate the influence of bacterial viability and opsonization on phagosomal pH and phagosome-lysosome interaction. Infect. Immun. **64:**319–325.
24. **Pagan-Ramos, E., J. Song, M. McFalone, M. H. Mudd, and V. Deretic.** 1998. Oxidative stress response and characterization of the oxyR-ahpC and furA-katG loci in *Mycobacterium marinum*. J. Bacteriol. **180:**4856–4864.
25. **Prince, D. S., et al.** 1989. Infection with *Mycobacterium avium* complex in patients without predisposing conditions. New Engl. J. Med. **321:**863–868.
26. **Ramakrishnan, L., R. H. Valdivia, J. H. McKerrow, and S. Falkow.** 1997. *Mycobacterium marinum* causes both long-term subclinical infection and acute disease in the leopard frog (*Rana pipiens*). Infect. Immun. **65:**767–773.
27. **Sarmento, A., and R. Appelberg.** 1996. Involvement of reactive oxygen intermediates in tumor necrosis factor alpha-dependent bacteriostasis of *Mycobacterium avium*. Infect. Immun. **64:**3224–3230.
28. **Schaefer, W. B., C. L. Davis, and M. L. Cohn.** 1970. Pathogenicity of transparent, opaque, and rough variants of *Mycobacterium avium* in chickens and mice. Am. Rev. Respir. Dis. **102:**499–506.
29. **Shinnick, T. M., and R. C. Good.** 1994. Mycobacterial taxonomy. Eur. J. Clin. Microbiol. Infect. Dis. **13:**884–901.
30. **Sommers, H. M., and R. C. Good.** 1985. Mycobacterium, p. 225. *In* E. H. Lennette (ed.), Manual of clinical microbiology, 4th ed. ASM Press, Washington, D.C.
31. **Wright, P. W., and R. J. Wallace.** 1995. Syndromes, diagnosis and treatment of rapidly growing mycobacteria, p. 373–389. *In* M. D. Rossman and R. R. MacGregor (ed.), Tuberculosis: clinical management and new challenges. McGraw Hill, Inc., New York, N.Y.

Editor: S. H. E. Kaufmann